Podoplanin binds ERM proteins to activate RhoA and promote epithelial-mesenchymal transition

Ester Martín-Villar[1], Diego Megías[2], Susanna Castel[3], Maria Marta Yurrita[1], Senén Vilaró[3,*] and Miguel Quintanilla[1,‡]

[1]Instituto de Investigaciones Biomédicas Alberto Sols, Consejo Superior de Investigaciones Científicas (CSIC)-Universidad Autónoma de Madrid (UAM), 28029 Madrid, Spain
[2]Centro Nacional de Investigaciones Oncológicas, 28029 Madrid, Spain
[3]Departamento de Biología Celular, Universidad de Barcelona, 08028 Barcelona, Spain

*Author died on 4 December 2005 and this paper is published in his memory
‡Author for correspondence (e-mail: mquintanilla@iib.uam.es)

Accepted 9 August 2006
Journal of Cell Science 119, 4541-4553 Published by The Company of Biologists 2006
doi:10.1242/jcs.03218

Summary

Podoplanin is a small membrane mucin expressed in tumors associated with malignant progression. It is enriched at cell-surface protrusions where it colocalizes with members of the ERM (ezrin, radixin, moesin) protein family. Here, we found that human podoplanin directly interacts with ezrin (and moesin) in vitro and in vivo through a cluster of basic amino acids within its cytoplasmic tail, mainly through a juxtamembrane dipeptide RK. Podoplanin induced an epithelial-mesenchymal transition in MDCK cells linked to the activation of RhoA and increased cell migration and invasiveness. Fluorescence time-lapse video observations in migrating cells indicate that podoplanin might be involved in ruffling activity as well as in retractive processes. By using mutant podoplanin constructs fused to green fluorescent protein we show that association of the cytoplasmic tail with ERM proteins is required for upregulation of RhoA activity and epithelial-mesenchymal transition. Furthermore, expression of either a dominant-negative truncated variant of ezrin or a dominant-negative mutant form of RhoA blocked podoplanin-induced RhoA activation and epithelial-mesenchymal transition. These results provide a mechanistic basis to understand the role of podoplanin in cell migration or invasiveness.

Supplementary material available online at
http://jcs.biologists.org/cgi/content/full/119/21/4541/DC1

Key words: Podoplanin/PA2.26 antigen, Ezrin, RhoA, Epithelial-mesenchymal transition, Cell migration

Introduction

Epithelial to mesenchymal transition (EMT) represents a phenotypic conversion by which epithelial cells lose their polarity and cohesiveness and acquire migratory features characteristic of fibroblasts. EMTs are required for morphogenetic processes and tissue remodelling during development, but are also involved in pathological situations such as wound healing, inflammation and tumor invasion and metastasis (Bissell and Radisky, 2001; Thiery, 2002). A wide variety of biological agents from cytokines to transcription factors has been found to promote either cell scattering or EMT in cultured epithelial cells (Gotzmann et al., 2004). In a previous work, we reported that podoplanin, a small mucin-like transmembrane glycoprotein also known as PA2.26 antigen or T1α among other names, induced the conversion from an epithelial to a fibroblast-like morphology when ectopically expressed in keratinocytes (Scholl et al., 1999).

Podoplanin is expressed in a variety of normal cells and tissues, including mesothelia, certain types of epithelia, neuronal cells, osteocytes and endothelia of lymphatic capillaries (Rishi et al., 1995; Wetterwald et al., 1996; Williams et al., 1996; Scholl et al., 1999; Kotani et al., 2003; Schacht et al., 2005; Breiteneder-Geleff et al., 1997; Breiteneder-Geleff et al., 1999). Mice deficient for podoplanin die immediately after birth owing to respiratory failure caused by malformation of alveoli (Ramirez et al., 2003). The *podoplanin* null mice also show defects in the lymphatic pattern formation associated with congenital lymphedema, dilation of vessels and diminished lymphatic transport (Schacht et al., 2003). These data point to an important role for podoplanin in the development of the lung and lymphatic vascular system, but its precise biological function remains poorly understood.

Podoplanin expression is upregulated in different types of experimental and human tumors, including squamous cell carcinomas of the skin, lung, esophagus, cervix, larynx and oral cavity (Gandarillas et al., 1997; Martín-Villar et al., 2005; Schacht et al., 2005; Kato et al., 2005; Wicki et al., 2006), colorectal adenocarcinomas (Kato et al., 2003), testicular germ cell tumors (Kato et al., 2004; Schacht et al., 2005) and mesotheliomas (Chu et al., 2005). In squamous cell carcinomas, podoplanin expression is frequently restricted to the invasive front (Martín-Villar et al., 2005; Wicki et al., 2006), and in some tumors correlates with downregulation of the cell-cell adhesion protein E-cadherin (Martín-Villar et al., 2005). Confocal and immunoelectron microscopy studies aimed at studying its subcellular localization revealed that podoplanin is concentrated at actin-rich microvilli and plasma membrane projections, where it colocalizes with members of the ERM (ezrin, radixin, moesin) protein family (Scholl et al., 1999; Martín-Villar et al., 2005). ERM proteins link integral

membrane proteins to the cortical actin cytoskeleton and participate in signal transduction pathways that regulate cell motility and adhesion (Bretscher et al., 2002). The presence of podoplanin at cell-surface projections and the finding that ezrin and moesin, but not radixin, can be coimmunoprecipitated with podoplanin from cell lysates suggested that this glycoprotein is involved in motility processes (Scholl et al., 1999). Further studies showed a pro-migratory function for podoplanin, because its expression in immortalized or premalignant keratinocytes either stimulated cell scattering (Martín-Villar et al., 2005) or promoted an EMT associated with increased invasive and metastatic features (Scholl et al., 1999; Scholl et al., 2000). In both cases, podoplanin stimulated the formation of plasma membrane extensions concomitantly with a major reorganization of the actin cytoskeleton and redistribution of ezrin to cell-surface protrusions (Scholl et al., 1999; Martín-Villar et al., 2005). Taken together, these data suggested an involvement of podoplanin in cell migration and invasiveness during tumor progression. We reasoned that an important cue for this function should be its ability to reorganize the actin cytoskeleton through recruitment of ERM proteins.

In this article, we show that wild-type human podoplanin promotes a complete EMT in Madin-Darby canine kidney (MDCK) type-II epithelial cells, a well-characterized cellular model to analyze the molecular mechanisms of epithelial cell plasticity (Gotzmann et al., 2004). The key elements for podoplanin to promote this phenotypic conversion are its ability to interact with ERM proteins through a cluster of basic amino acids within its cytoplasmic tail and the regulation of RhoA GTPase activity.

Results

The binding of podoplanin to ERM proteins requires a juxtamembrane cluster of basic amino acids.

The 162 amino acid human podoplanin molecule contains an ectodomain (EC) with a high proportion of O-glycosylated S and T residues, a membrane-spanning domain (TM) and a short cytoplasmic tail (CT) of only nine amino acids (Fig. 1). The TM and CT domains are highly conserved across species (Zimmer et al., 1999; Martín-Villar et al., 2005; Kaneko et al., 2006). Within the CT domain the only obvious functional motif is a cluster of basic amino acids (Fig. 1, bold) shared by transmembrane proteins of the microvillus that has been shown to be involved in direct binding to ERM proteins (Yonemura et al., 1998). However, although coimmunoprecipitation experiments suggested an association of podoplanin with ezrin and moesin (Scholl et al., 1999), no proof for a direct interaction of the podoplanin endodomain with these cytoskeletal linkers exists. To analyze whether podoplanin binds ERM proteins directly through this cluster of basic residues, we expressed the wild-type cytoplasmic tail of human podoplanin (PCT) as a fusion protein with glutathione-S-transferase (GST), and tested whether the substitution of positively charged residues (RK…R) by uncharged polar amino acids (see Fig. 1) affected the interaction of PCT with purified recombinant full-length ezrin and moesin or their N-terminal sequences (N-ERMAD domains). Although both controls (GST-Sepharose and uncoupled Sepharose) bound some ezrin and moesin, the interaction of these proteins with GST-PCT was clearly increased over the non-specific background (Fig. 2A). The same occurred with the CT of the cell-surface receptor CD44, used in this experiment as a positive control (Hirao et al., 1996; Legg and Isacke, 1998; Yonemura et al., 1998). Phosphatidylinositol 4,5-bisphosphate (PIP_2), a positive regulator of ERM binding to membrane proteins (Bretscher et al., 2002), enhanced the interaction of ezrin and moesin with the CTs of both podoplanin and CD44 (data not shown), as demonstrated previously for CD44 (Hirao et al., 1996). Mutation of one (PCT.N), two (PCTQN) or all three (PCTQN.N) basic amino acids highly decreased the binding of PCT to ezrin and moesin, although PCT.N (in which only the most C-terminal R159 was mutated) appeared to conserve some specific binding activity, particularly to moesin. These data indicate that the motif RK…R within the podoplanin endodomain is able to interact directly with ERM proteins in vitro.

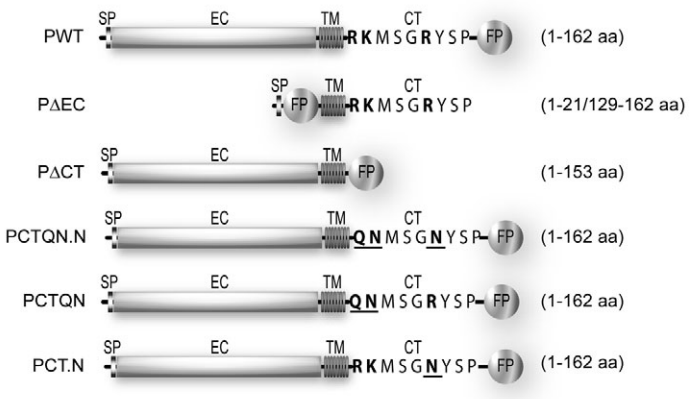

Fig. 1. Schematic representation of podoplanin fusion constructs used for transfection. Numbers indicate podoplanin amino acid sequences (Martín-Villar et al., 2005) conserved in the construct. CT, cytoplasmic domain; EC, ectodomain; FP, fluorescent protein (EYFP or EGFP) used for the experiments specified in the text; SP, signal peptide; TM, transmembrane domain. Basic amino acids (bold) within the CT domain were substituted by uncharged polar residues (bold and underlined).

To ascertain whether this cluster of basic residues mediates the binding of podoplanin to ERM proteins in vivo, we engineered several constructs encoding wild-type or mutant podoplanin proteins fused to enhanced yellow fluorescent protein (EYFP). Mutant proteins were obtained that lacked the cytoplasmic tail (PΔCT) or in which the juxtamembrane cluster of basic amino acids was substituted by uncharged polar residues, as above (see Fig. 1). Wild-type podoplanin (PWT) and the mutant constructs fused to EYFP were cotransfected with enhanced cyan fluorescent protein (ECFP)-tagged ezrin in MDCK type-II cells and the interaction between ezrin and podoplanin proteins determined by fluorescence resonance energy transfer (FRET). In contrast to MDCK type-I cells, MDCK type-II cells do not express endogenous podoplanin (Zimmer et al., 1999) (our own results). FRET efficiency ($FRET_{eff}$) between EYFP-tagged podoplanin constructs and ECFP-tagged ezrin was monitored by acceptor photobleaching in different cells and cell regions (Fig. 2C-E). The mean $FRET_{eff}$ value for wild-type podoplanin was 27.1%, indicating that a substantial proportion of PWT is complexed with ezrin in vivo. $FRET_{eff}$ decreased to about 5.9% in cells expressing PCT.N, whereas $FRET_{eff}$ values fall to zero in cells expressing mutant PΔCT, PCTQN.N and PCTQN (Fig. 2B). These results

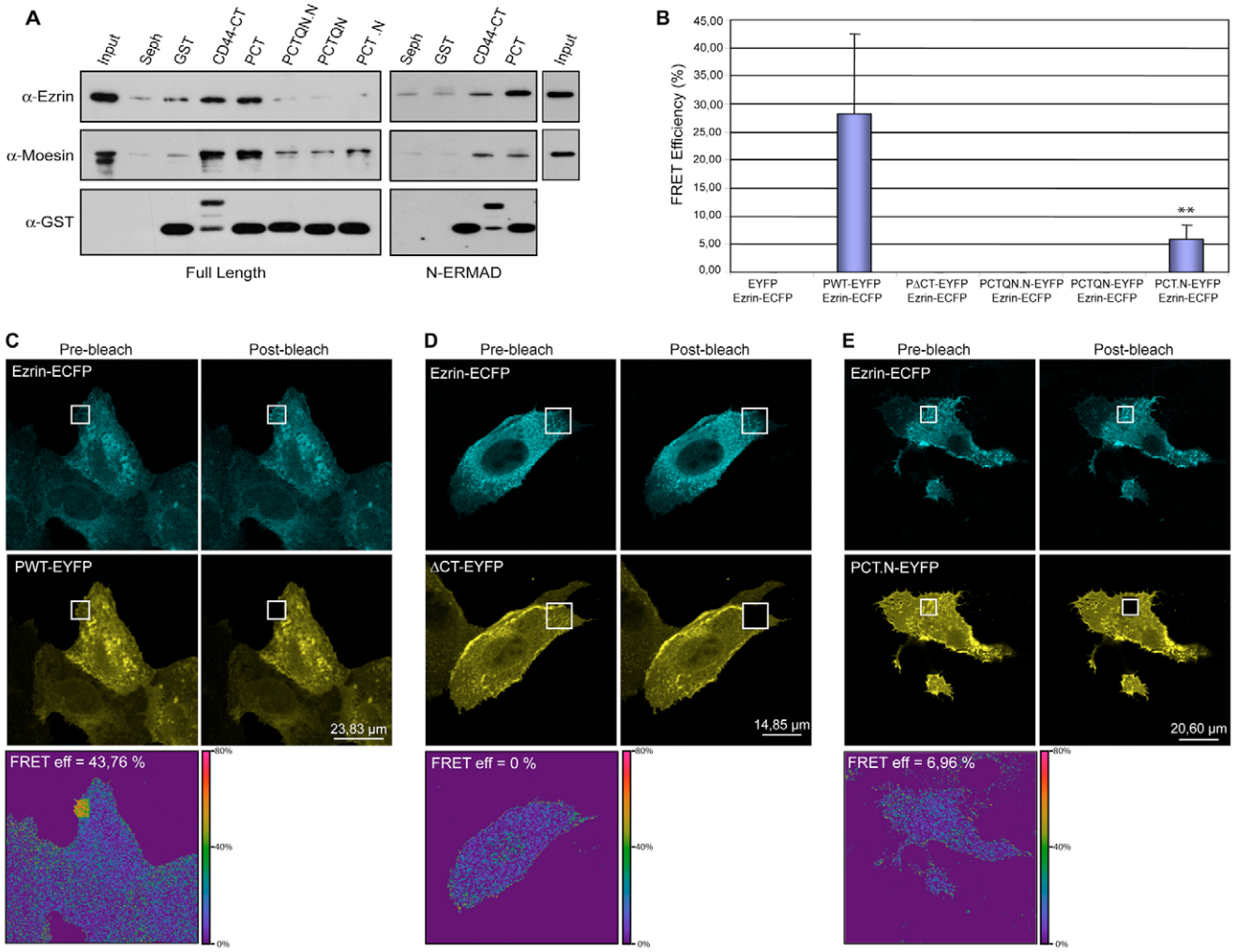

Fig. 2. Podoplanin binds to ERM proteins through a cluster of basic amino acids within its cytoplasmic tail. (A) Association of ezrin and moesin with podoplanin CT. GST and GST fusion proteins bound to Sepharose beads were incubated with purified recombinant full-length ezrin or moesin or their N-ERMADs. Proteins bound to the beads were fractionated by SDS-PAGE followed by western blotting using anti-ezrin or anti-moesin antibodies. CD44-CT was used as a positive control. (B) $FRET_{eff}$ values for cells coexpressing EYFP/Ezrin-ECFP (n=5), PWT-EYFP/Ezrin-ECFP (n=14), PΔCT-EYFP/Ezrin-ECFP (n=7), PCTQN.N-EYFP/Ezrin-ECFP (n=7), PCTQN-EYFP/Ezrin-ECFP (n=6) and PCT.N-EYFP/Ezrin-ECFP (n=10). Note the significant reduction (**P<0.01) of $FRET_{eff}$ in PCT.N with respect to PWT and the absence of FRET in PCTQN.N, PCTQN and PΔCT cell transfectants. (C-E) Confocal fluorescence images showing acceptor photobleaching FRET analysis in MDCK cell transfectants. Images of representative cells coexpressing Ezrin-ECFP with PWT-EYFP (C), PΔCT-EYFP (D) or PCT.N-EYFP (E) are shown. ECFP and EYFP emission signals were collected before (left panels) and after (right panels) EYFP photobleaching in the boxed regions. An increased ECFP fluorescence signal after photobleaching indicates FRET. The $FRET_{eff}$ is represented in the bottom panel on a pseudocolor cell map with scale shown on the right.

demonstrate that in vivo association of podoplanin with ezrin is mainly mediated by the juxtamembrane dipeptide RK. Mutation of the most C-terminal residue R159 significantly impaired but did not prevent this association.

Podoplanin induces an EMT in MDCK cells through the cytoplasmic domain

In a preliminary test in which the wild-type human podoplanin cDNA cloned into the pcDNA3 expression vector (Martín-Villar et al., 2005) was stably expressed in MDCK type-II cells, we found a dramatic change from an epithelial to a fibroblast-like morphology (data not shown). Therefore, to investigate which region of the molecule is required to promote this morphological change, PWT and the mutant constructs fused to enhanced green fluorescent protein (EGFP), including one that lacked the ectodomain (PΔEC, see Fig. 1), were stably expressed in MDCK cells. All selected clones expressing PWT, PΔEC or PCT.N exhibited a clear fibroblastic morphological appearance. By contrast, cells expressing PΔCT, PCTQN.N and PCTQN maintained the epithelial morphology, as did control clones expressing EGFP alone (EGFP). Two clones of each construct were then selected for further studies. The total level of podoplanin expression and the size of the exogenous proteins were analyzed by western blotting (Fig. 3A). We also monitored the expression of differentiation protein markers. Fibroblastic clones induced by PWT and PΔEC had lost the expression of epithelial markers, such as E-cadherin. They also synthesized reduced levels of cytokeratin 8, β-catenin and

p120 catenin (ctn) isoform 3 (the main p120 ctn form expressed in epithelial MDCK cells) (Sarrio et al., 2004). Conversely, these cells had increased expression of N-cadherin, p120 ctn isoform 1 and fibronectin (Fig. 3A): all mesenchymal markers upregulated during EMT (Cavallaro and Christofori, 2004; Sarrio et al., 2004). Epithelial MDCK cells expressing PCTQN.N and PCTQN retained E-cadherin and cytokeratin levels and did not switch to expression of N-cadherin. Interestingly, clones expressing PCT.N, despite their fibroblastic morphology, retained expression of E-cadherin (although at a reduced level in clone 1), p120 ctn isoform 3 and cytokeratin 8, whereas expression of N-cadherin and p120 ctn isoform 1 was upregulated (Fig. 3A). These data indicated that MDCK cells expressing PCT.N have an intermediate phenotype between epithelial and mesenchymal (which we have termed fibroblastoid). No substantial change in the expression levels of mesenchymal vimentin was observed in the different clones regardless of their epithelial or fibroblastic morphology. Nevertheless, vimentin, which is already significantly expressed in MDCK cells (Peinado et al., 2003) (see also Fig. 3A), was better organized in a clear filament network in fibroblast-like cells induced by PWT and PΔEC in comparison to epithelial cell clones (Fig. S1 in supplementary material). As expected, PCT.N-MDCK cells were positively stained for E-cadherin, but the protein was relocated from cell-cell contacts to the cytoplasm, indicating a loss of E-cadherin function at cell-cell junctions (Fig. S1 in supplementary material). A summary of the phenotypic changes produced in MDCK cells by wild-type and mutant podoplanin proteins is presented in Table 1.

RT-PCR analysis showed that loss of E-cadherin expression in PWT and PΔEC cell transfectants occurred at the transcriptional level (Fig. 3B). Since several transcription repressors of E-cadherin, such as the zinc finger factors Snail and Slug, have been found to promote EMT (Cano et al., 2000; Batlle et al., 2000; Bolós et al., 2003), and Snail appears to be involved in the EMT induced by TGF-β_1 in MDCK cells (Peinado et al., 2003), we analyzed the mRNA levels of these transcription factors in the transfectants. No clear correlation could be established between the mRNA transcript levels and the level of E-cadherin expression or the phenotype of the different cell clones, suggesting that podoplanin-induced EMT did not involve upregulation of Snail or Slug transcription factors.

In summary, these results indicate that expression of wild-type podoplanin in MDCK cells induces a complete EMT associated with reprogramming of differentiation-related gene expression. The crucial region of the molecule involved in this transition appears to be the cluster of basic residues within the cytoplasmic tail responsible for binding to ERM proteins, particularly the juxtamembrane dipeptide RK.

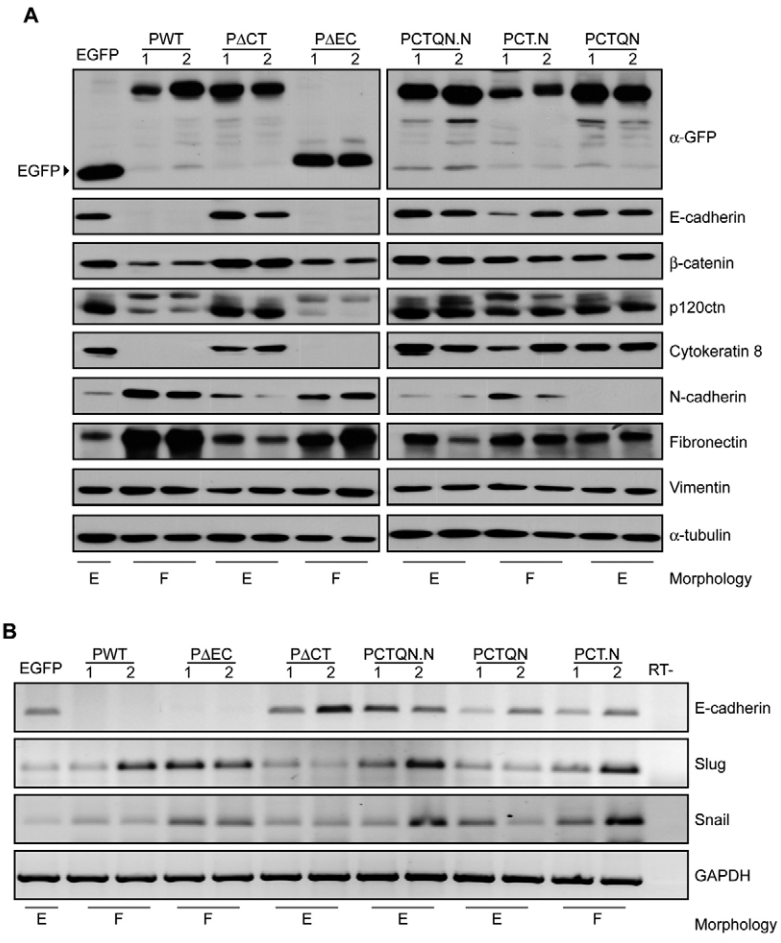

Fig. 3. MDCK cells expressing podoplanin undergo an EMT that depends on the cytoplasmic domain. (A) Western blot analysis of podoplanin proteins and of differentiation-related markers in MDCK-derived cell clones expressing EGFP (control) and PWT, PΔCT, PΔEC, PCTQN.N, PCTQN or PCT.N fusion proteins. (B) Expression of E-cadherin, Snail and Slug mRNA transcripts by RT-PCR. *GAPDH* was amplified as a control for the amount of cDNA present in each sample. The RT- lane shows the results of amplification in the absence of cDNA. The morphology of the cell transfectants is indicated below (E, epithelial; F, fibroblastic).

Localization of podoplanin at cell-surface protrusions does not require the cytoplasmic tail or the ectodomain

The subcellular localization of wild-type and mutant podoplanin proteins was analyzed by confocal microscopy. To determine the fraction of the exogenous protein that was specifically directed to the cell surface, we performed a comparison between the fluorescence signal due to EGFP and the signal obtained after in vivo pre-embedding staining (at 4°C) using either a specific antibody recognizing the podoplanin ectodomain (Martín-Villar et al., 2005) or an anti-EGFP antibody (for detection of PΔEC). As shown in Fig. 4, PWT was distributed all along the plasma membrane concentrated at cell-surface protrusions (microvilli, filopodia and ruffles), as previously reported (Scholl et al., 1999; Martín-Villar et al., 2005). Patchy staining was also seen in the cytoplasm, indicating the presence of podoplanin at internal membrane structures (see below). Deletion of the ectodomain did not alter this pattern of expression, although the amount of PΔEC directed to the cell surface was substantially

Table 1. Summary of the phenotypic changes induced by podoplanin constructs in MDCK cells

Construct	Morphology	E-CD	N-CD	p120 ctn i.3	p120 ctn i.1	K8	Fn	Cell migration (wound healing)	Invasiveness (Matrigel)	RhoA activity (cell lysates)
Control (EGFP)	Epithelial	+	+/–	++	–	+	+	Collective/Slow	–	–
PWT	Fibroblastic (well spread)	–	++	+/–	+	–	++	Individual/Fast	++	+
PΔEC	Fibroblastic (elongated)	–	++	+/–	+	–	++	Individual/Fast	++	+
PΔCT	Epithelial	+	+/–	++	–	+	+	Mixed/Intermediate	+	–
PCTQN.N	Epithelial	+	+/–	++	–	+	+	Collective/Slow	–	–
PCTQN	Epithelial	+	–	++	–	+	+	Collective/Slow	–	–
PCT.N clone 1	Fibroblastic (elongated)	+/–	++	+	+	+	+	Individual/Fast	++	+
PCT.N clone 2	Fibroblastic (elongated)	+	+	+	+	+	+	Individual/Fast	++	+/–

CD, cadherin; ctn, catenin; Fn, fibronectin; K, cytokeratin.

reduced with respect to PWT, because a significant fraction of the truncated molecule had a perinuclear location, probably concentrated at the Golgi apparatus. Interestingly, neither deletion of the cytoplasmic tail nor mutation of the ERM-binding sites prevented localization of the mutant proteins at cell-surface protrusions: PΔCT, PCTQN.N and PCTQN proteins localized on the apical and lateral surfaces of polarized epithelial MDCK cells, concentrated at microvilli and cell-cell junctions (Fig. 4). On the other hand, the subcellular distribution of mutant PCT.N did not differ significantly from that of PWT. These results suggest that neither the ectodomain nor the association of podoplanin with the cytoskeleton through the cytoplasmic tail is required for localization of podoplanin at cell-surface protrusions.

We also studied the organization of the actin cytoskeleton in the cell transfectants (Fig. S2 in supplementary material). Epithelial MDCK cells transfected with mutant PΔCT, PCTQN.N and PCTQN showed strong cortical actin bundles and short thin stress fibers: the same pattern exhibited by the parental cell line and control clones. These cells also showed small vinculin-containing focal contacts. In cells expressing PWT, PΔEC or PCT.N, however, a reorganization of the actin cytoskeleton concomitantly with the induced morphological changes was observed. Thus, cortical actin bundles disappeared in these fibroblast-like cells,

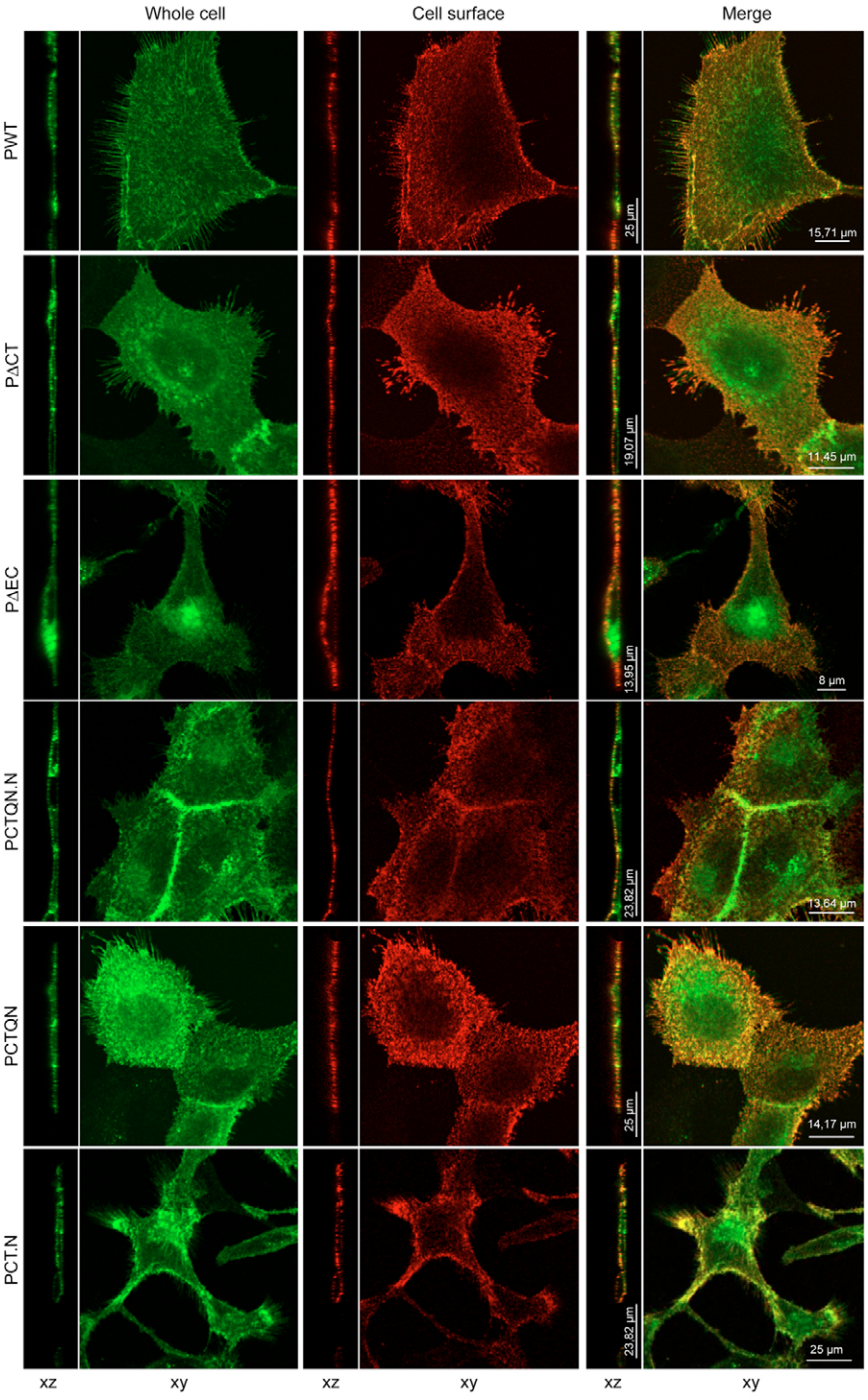

Fig. 4. Subcellular localization of wild-type and mutant podoplanin proteins. Confocal images of horizontal (*x*-*y*) and vertical (*x*-*z*) sections of MDCK cells expressing the indicated podoplanin proteins fused to EGFP are shown. The exogenous proteins specifically expressed at the cell surface were detected by in vivo pre-embedding staining using antibodies either recognizing the podoplanin EC domain or EGFP (for detection of PΔEC).

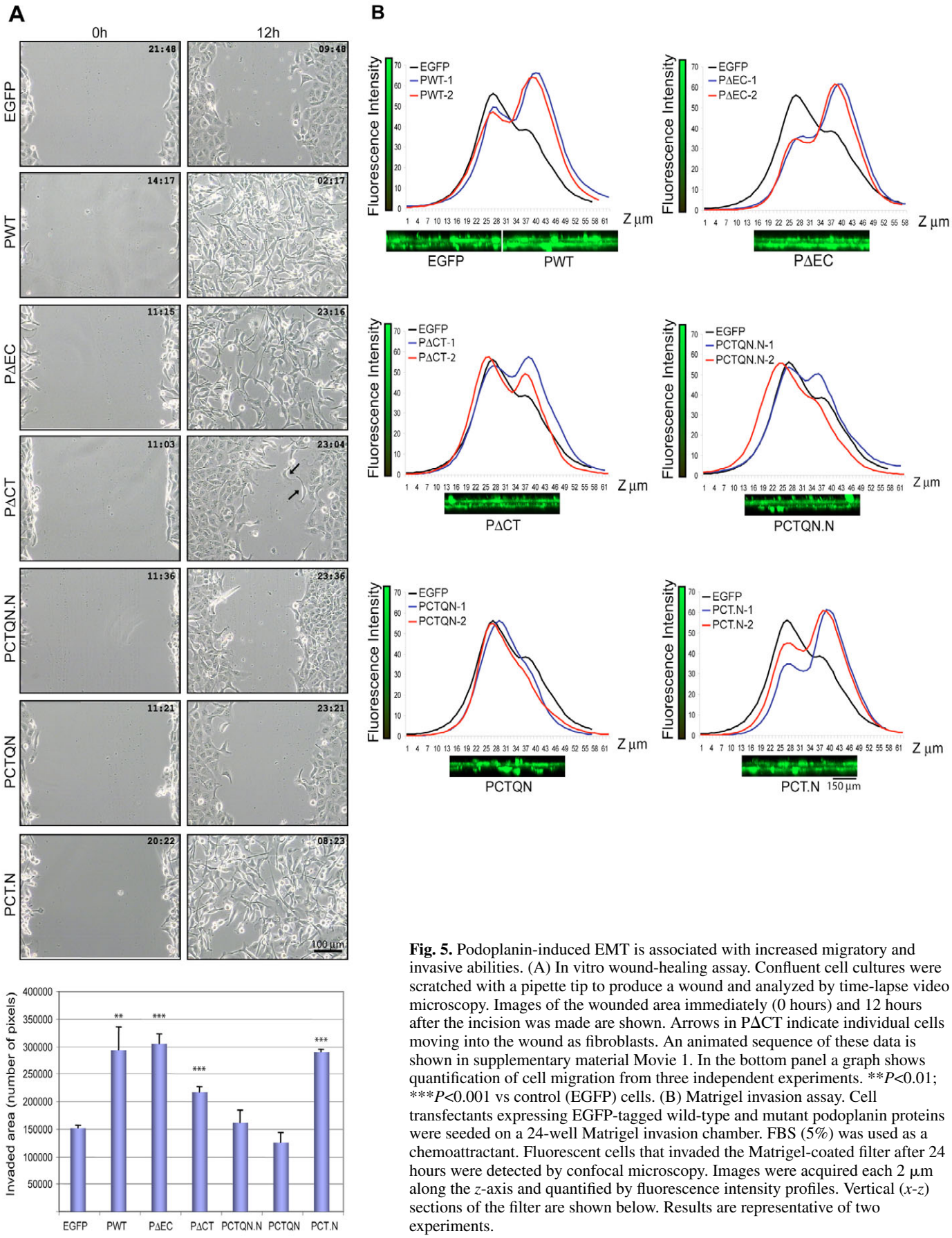

Fig. 5. Podoplanin-induced EMT is associated with increased migratory and invasive abilities. (A) In vitro wound-healing assay. Confluent cell cultures were scratched with a pipette tip to produce a wound and analyzed by time-lapse video microscopy. Images of the wounded area immediately (0 hours) and 12 hours after the incision was made are shown. Arrows in PΔCT indicate individual cells moving into the wound as fibroblasts. An animated sequence of these data is shown in supplementary material Movie 1. In the bottom panel a graph shows quantification of cell migration from three independent experiments. $^{**}P<0.01$; $^{***}P<0.001$ vs control (EGFP) cells. (B) Matrigel invasion assay. Cell transfectants expressing EGFP-tagged wild-type and mutant podoplanin proteins were seeded on a 24-well Matrigel invasion chamber. FBS (5%) was used as a chemoattractant. Fluorescent cells that invaded the Matrigel-coated filter after 24 hours were detected by confocal microscopy. Images were acquired each 2 μm along the *z*-axis and quantified by fluorescence intensity profiles. Vertical (*x*-*z*) sections of the filter are shown below. Results are representative of two experiments.

whereas F-actin accumulated at lamellipodia and ruffles. Nevertheless, well-spread PWT-MDCK fibroblasts showed more-pronounced focal contacts and longer and thicker stress fibers than elongated MDCK cells expressing PΔEC or PCT.N (Fig. S2 in supplementary material).

Dynamics of migration in MDCK cells expressing wild-type and mutant podoplanin proteins

To examine whether the observed phenotypic changes in MDCK cell transfectants were associated with increased motility, we performed an in vitro wound-healing assay. PWT- and PΔEC-MDCK cells were able to repopulate a wound made 12 hours earlier in a confluent culture, whereas closure of the wounds made in MDCK or control cell cultures was less than 50% (Fig. 5A). PCT.N-MDCK cells also had high migratory abilities, comparable with those of cells expressing PWT and PΔEC. Time-lapse video observations showed that fibroblast-like PWT-, PΔEC- and PCT.N-MDCK cells migrated individually, extending and retracting protrusions and continually changing their orientations and shapes (Fig. 5A and Movie 1 in supplementary material). By contrast, epithelial cells expressing PCTQN.N and PCTQN migrated collectively, maintaining cell-cell contacts (Fig. 5A and Movie 1 in supplementary material) following the principles reported for migration of parental MDCK cells (Matsubayashi et al., 2004; Faroqui and Fenteany, 2005). Surprisingly, epithelial PΔCT-MDCK cells exhibited an intermediate behavior, in which migration was significantly reduced when compared with fibroblast-like cell lines, but those cells migrated faster than the other epithelial cell transfectants. The dynamics of cell migration in PΔCT-MDCK wounds were similar to those described for control cells, although in this case the speed of movement was higher and contacts between marginal cells and their following neighbours became weaker, resulting in numerous individual cells moving as fibroblasts into the wound (arrows in Fig. 5A and Movie 1 in supplementary material).

We also studied the ability of the cell transfectants to invade into a reconstituted basement membrane (Matrigel). Invasiveness was highly enhanced in fibroblast-like PWT-, PΔEC- and PCT.N-MDCK cells with respect to epithelial cells expressing PCTQN.N, PCTQN and control clones (Fig. 5B). As in the in vitro wound-healing assay, PΔCT-MDCK cells showed an intermediate behavior between those two groups of transfectants.

Fluorescence time-lapse confocal microscopy on isolated MDCK cells expressing wild-type or mutant podoplanin proteins fused to EGFP allowed us to visualize the dynamics of the subcellular distribution of podoplanin during cell locomotion (Fig. 6 and Movies 3-5 in supplementary material). PWT was present at the edge of lamellipodial extensions, but it disappeared from attached lamellipodia (asterisk) whereas it remained on the top of ruffles moving centripetally across the cell surface. In addition, podoplanin clustered at the cell tail (arrowhead) before the rearmost adhesions to the substratum

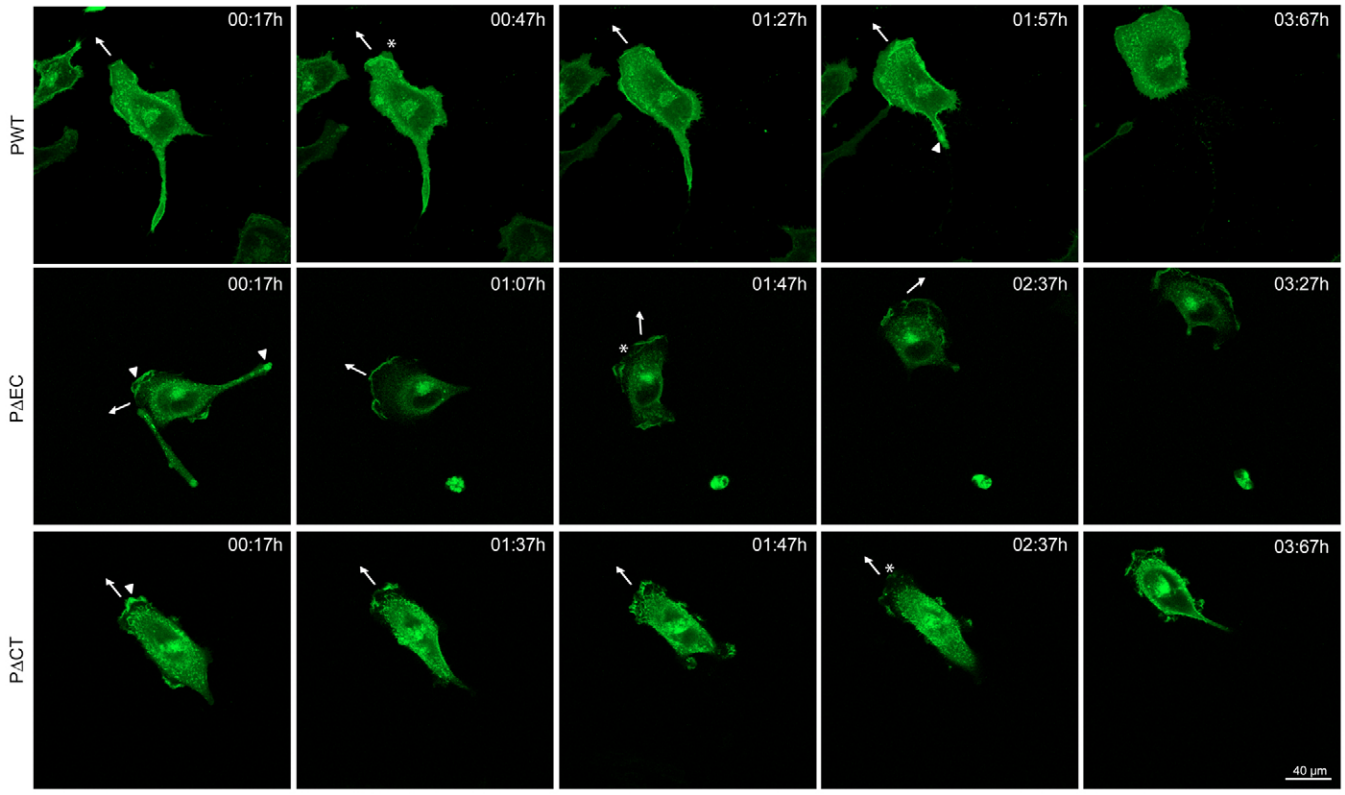

Fig. 6. Dynamics of podoplanin subcellular localization during cell locomotion. Isolated MDCK cells expressing EGFP-tagged PWT, PΔEC and PΔCT proteins were imaged by capturing sections of 0.5 μm every 10 minutes for 4 hours. Images in all panels correspond to 3D reconstructions. Arrowheads indicate podoplanin fluorescence signal concentrated at the leading edge of lamellipodial extensions and on the retracting tail, whereas asterisks indicate loss of fluorescence signal on lamellipodial extensions attached to the substratum. The direction of cell migration is indicated by arrows. Animated sequences of these data are shown in supplementary material Movies 3-5.

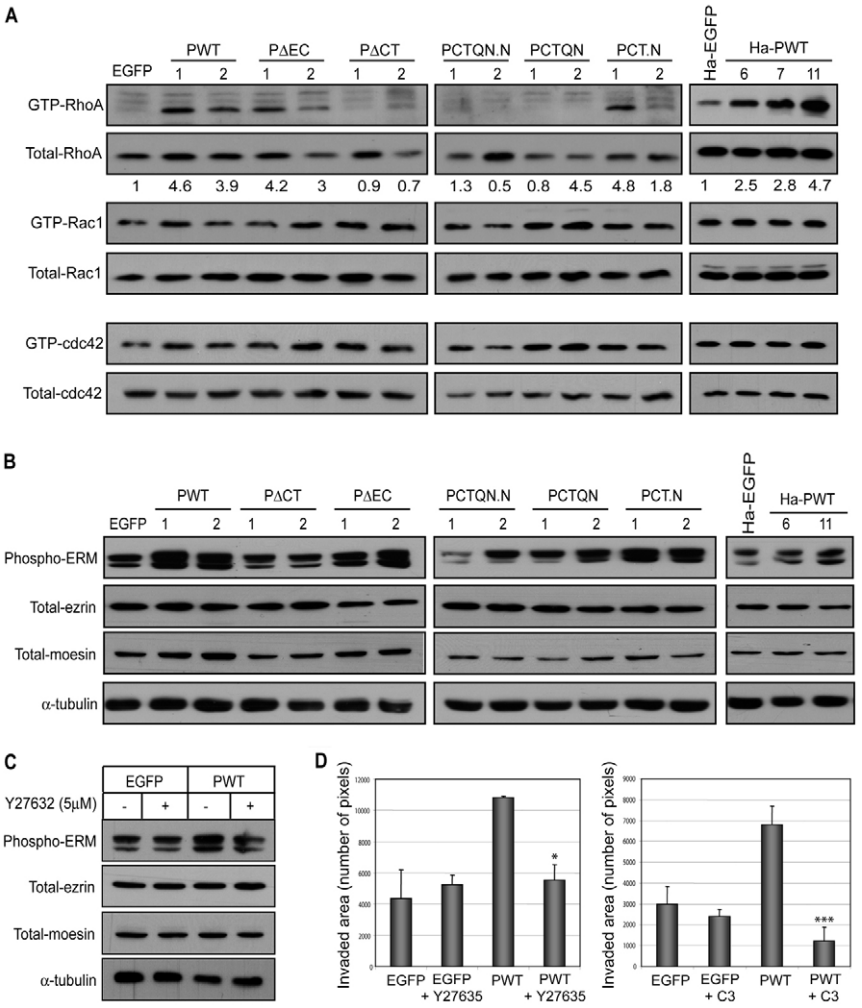

Fig. 7. Podoplanin-induced EMT is associated with upregulation of RhoA activity. (A) Rho, Rac and Cdc42 bound to GTP affinity pull-down assays were used to determine the levels of active Rho GTPases. Levels of active RhoA, Rac1 and Cdc42 in MDCK and HaCaT cell clones transfected with the empty vector (EGFP) and with wild-type and mutant podoplanin constructs fused to EGFP. Quantification of RhoA-GTP expression level relative to total RhoA level was performed by densitometric analysis. Values below blots are relative to control (EGFP) cells, to which an arbitrary value of 1 was given. Results are representative of two experiments. (B) Western blot analysis of ERM phosphorylation relative to the total expression levels of ezrin and moesin. The levels of α-tubulin were determined as a control for protein loading. (C) Western blot analysis of phospho-ERM levels relative to the total expression levels of ezrin and moesin in MDCK cells transfected with the empty vector (EGFP) and PWT before and after treatment with the Rock inhibitor Y27632. (D) Inhibition of RhoA signaling blocks podoplanin-stimulated cell migration. In vitro wound-healing assays of control (EGFP) and PWT-MDCK cells were performed (as in Fig. 5A) in the absence or presence of either Y27632 (which inhibits Rock) or soluble C3 transferase (which inhibits RhoA, RhoB and RhoC). Y27632 and C3 transferase reduced PWT-MDCK cell migration to basal and below basal levels, respectively. *P<0.05; ***P<0.001 vs PWT-MDCK cells.

disassembled and the tail retracted. These observations suggest that podoplanin might be involved in ruffling activity as well as in retractive processes. A substantial amount of podoplanin was also seen associated with internal membranous structures (probably the Golgi system) and on the surface of vesicles located close to the plasma membrane or surrounding the Golgi apparatus (see Movie 2 in supplementary material). The importance of this latter observation remains to be investigated. No significant change was observed in the distribution of mutant PΔEC (or PCT.N) with respect to PWT during cell locomotion, although migration of PΔEC-MDCK cells was rather erratic compared with directional movement of PWT-MDCK cells (Fig. 6; Movies 3 and 5 in supplementary material). On the other hand, mutant PΔCT (as well as PCTQN.N and PCTQN) concentrated at ruffles and microvilli, although ruffling activity was less intense in these epithelial cell transfectants (Movie 4 in supplementary material) compared with fibroblast-like cells expressing PWT, PΔEC or PCT.N.

Podoplanin-induced EMT involves increased RhoA activity

Rho GTPases have been found to mediate cytoskeletal rearrangements and have been implicated in cell migration and invasiveness (Ridley, 2001; Sahai and Marshall, 2002a). To ascertain whether podoplanin-induced EMT involved regulation of Rho GTPases activity, we used biochemical pull-down assays to analyze the activation state of RhoA, Rac1 and Cdc42 in the cell transfectants. While in parental MDCK cells or control clones the overall level of active RhoA (RhoA-GTP) was almost undetectable (Zondag et al., 2000), the activity of RhoA was dramatically increased in fibroblastic clones expressing PWT and PΔEC (Fig. 7A). Enhanced activation of RhoA was also found in fibroblastoid PCT.N-MDCK cells, although in this case the level of active RhoA varied between the two different clones (clone 1 showed higher RhoA-GTP levels than clone 2). Lysates from epithelial cells transfected with PΔCT, PCTQN.N and PCTQN did not show significant changes in RhoA activation over basal levels (Fig. 7A and Table 1). In all cases, there was little change in the total level of expression of RhoA in each of the transfectants after correcting for protein levels with α-tubulin (data not shown), indicating that activation of RhoA was not due to an increase in its expression levels. In contrast to RhoA, the levels of active Rac1 and Cdc42 did not vary substantially in any of the transfectants with respect to control cells. PWT alone (without EGFP) was also able to activate RhoA specifically without changing the levels of active Rac1 and Cdc42 (data not shown), indicating that this effect is not due to EGFP modification. On the other hand, we confirmed that the ability of podoplanin to activate RhoA specifically is not dependent on a particular cell line, because immortalized HaCaT keratinocytes

expressing PWT also showed increased RhoA-GTP levels whereas the levels of Rac1 and Cdc42 bound to GTP remained unchanged (Fig. 7A). Double immunofluorescence confocal microscopy analysis revealed that both RhoA and Rac1, but not Cdc42, colocalized with podoplanin at cell-surface protrusions in fibroblast-like MDCK cells expressing PWT, PΔEC, and PCT.N (Fig. S3 in supplementary material and data not shown). These results might indicate local activation of both RhoA and Rac1 at podoplanin-induced filopodia and ruffles even though no change in the activity of Rac1 was observed in whole-cell lysates.

Since RhoA-associated kinase (Rock), a downstream effector of RhoA, has been shown to phosphorylate and activate ERM proteins (Matsui et al., 1998), we analyzed the status of ERM phosphorylation in the cell transfectants (Fig. 7B). Increased levels of phospho-ERM proteins were found in fibroblastic and fibroblastoid clones with respect to control cells and epithelial cell transfectants. MDCK cells transfected with PWT alone (without EGFP) and HaCaT keratinocytes expressing PWT also showed enhanced phospho-ERM levels (Fig. 7B). Treatment of PWT-MDCK cells with the Rock inhibitor Y27632 reduced ERM phosphorylation to basal levels, whereas the inhibitor did not affect ERM phosphorylation in control cells (Fig. 7C). These results confirm that podoplanin stimulation of ERM phosphorylation is mediated by RhoA-dependent activation of Rock. Moreover, inhibition of either Rock with Y27632 or RhoA with the exoenzyme C3 transferase blocked podoplanin-stimulated cell migration (Fig. 7D).

Taken together, these results suggest that to activate RhoA, podoplanin needs to recruit ERM proteins through its ERM-binding site. Upregulation of RhoA activity leads to Rock-mediated ERM phosphorylation and stabilization of ERM proteins in an open, active conformation (Matsui et al., 1998), which further strengthens the anchorage of podoplanin to the cytoskeleton, allowing EMT and enhanced cell migration and invasion. Therefore, we reasoned that podoplanin-induced EMT should be prevented by inhibiting the function of either ezrin or RhoA.

Blocking ezrin or RhoA prevents podoplanin-induced EMT

In order to analyze the effects of the functional loss of ezrin or RhoA in podoplanin-mediated EMT, MDCK cells were cotransfected with PWT and a construct encoding a dominant-negative form of either ezrin or RhoA. The N-terminal domain of ezrin (N-ezrin) tagged with vesicular stomatitis virus glycoprotein G (VSVG) (Crepaldi et al., 1997) and a hemagglutinin (HA)-tagged N19RhoA mutant form were used to suppress ezrin and RhoA functions, respectively. The results of these experiments are shown in Fig. 8. When coexpressed together with one of these dominant-negative forms, podoplanin was unable to upregulate RhoA activity (Fig. 8C) and to promote EMT (Fig. 8A,B). Loss of function of ezrin or RhoA also suppressed podoplanin stimulation of phospho-ERM levels (Fig. 8C). These results demonstrated that ezrin and RhoA play crucial roles in podoplanin-mediated EMT.

Discussion

We show in this work that expression of human podoplanin in epithelial MDCK cells promotes a complete EMT linked to downregulation of epithelial genes (E-cadherin, p120 ctn isoform 3 and cytokeratin 8) and upregulation of mesenchymal markers (N-cadherin, p120 ctn isoform 1 and fibronectin). This conversion allowed MDCK cells to acquire migratory features, including a switch from a relatively slow collective pattern of cell migration to a faster, individualized cell locomotion pattern during wound healing, and increased invasiveness through Matrigel. In several human cancer types, downregulation of E-cadherin expression is accompanied by upregulation of mesenchymal N-cadherin, and this cadherin switch also occurs during EMTs in embryonic development. N-cadherin appears to exert the opposite effect to that of E-cadherin, because it promotes cell migration or invasion instead of cell-cell cohesion (reviewed by Cavallaro and Christofori, 2004). Interestingly, in podoplanin-induced EMT the E- to N-cadherin switch correlates with a change in the expression of p120 ctn isoforms from isoform 3 to isoform 1. Although this p120 ctn switch was previously observed in EMTs induced in MDCK cells by the E-cadherin transcriptional repressors Snail and Slug (Sarrio et al., 2004), no correlation was found between the levels of these transcription factors and the expression of p120 ctn isoform 1 in podoplanin-induced EMT, indicating that changes from p120 ctn isoform 3 to isoform 1 and from E- to N-cadherin do not necessarily involve upregulation of Snail or Slug.

As also shown in this study, podoplanin induces upregulation of RhoA activity in MDCK and HaCaT cells. Since podoplanin promoted cell scattering, but not a complete EMT in HaCaT keratinocytes (Martín-Villar et al., 2005), these results indicate that podoplanin-induced RhoA activation in epithelial cells precedes EMT rather than being a consequence of it. Several reports have implicated RhoA in epithelial tumor progression in vivo and in vitro (reviewed by Sahai and Marshall, 2002a; Lozano et al., 2003). Thus, elevation of RhoA activity has been found to result in disruption of adherens junctions and EMT in colon carcinoma cells (Sahai and Marshall, 2002b), TGF-β_1-stimulated mammary epithelial cells (Bhowmick et al., 2001) and Rac1-activated epithelial-like NIH3T3 cells (Sander et al., 1999). Epithelial MDCK cells are characterized by high Rac1 and low RhoA activity, and downregulation of Rac1 activity by oncogenic Ras also leads to increased RhoA activity and EMT (Zondag et al., 2000). The fact that podoplanin is able to activate RhoA without affecting Rac1 or Cdc42 activity suggests a direct link between podoplanin expression and RhoA activation in MDCK cells, but does not exclude a role for Rac1 or Cdc42 in podoplanin-mediated cell motility. In fact, Rac1 colocalizes with podoplanin at cell-surface protrusions in podoplanin-induced MDCK fibroblastic cells. Whereas Rac1 and Cdc42 have been involved in the establishment and maintenance of epithelial intercellular adhesions and are respectively required for lamellipodium and filopodium extensions in migrating cells, RhoA is implicated in the generation of contractile force, and in moving the body and tail of the cell behind the leading edge (Ridley, 2001). As podoplanin clusters on the cell tail just before tail retraction is completed, it would have a direct role in retractive processes by activating RhoA on the trailing edge.

The crucial podoplanin structural motif involved in RhoA activation and EMT seems to reside in the endodomain, because its deletion (PΔCT) prevented upregulation of RhoA activity and halted conversion to a fibroblast-like phenotype, whereas deletion of the ectodomain (PΔEC) did not. The

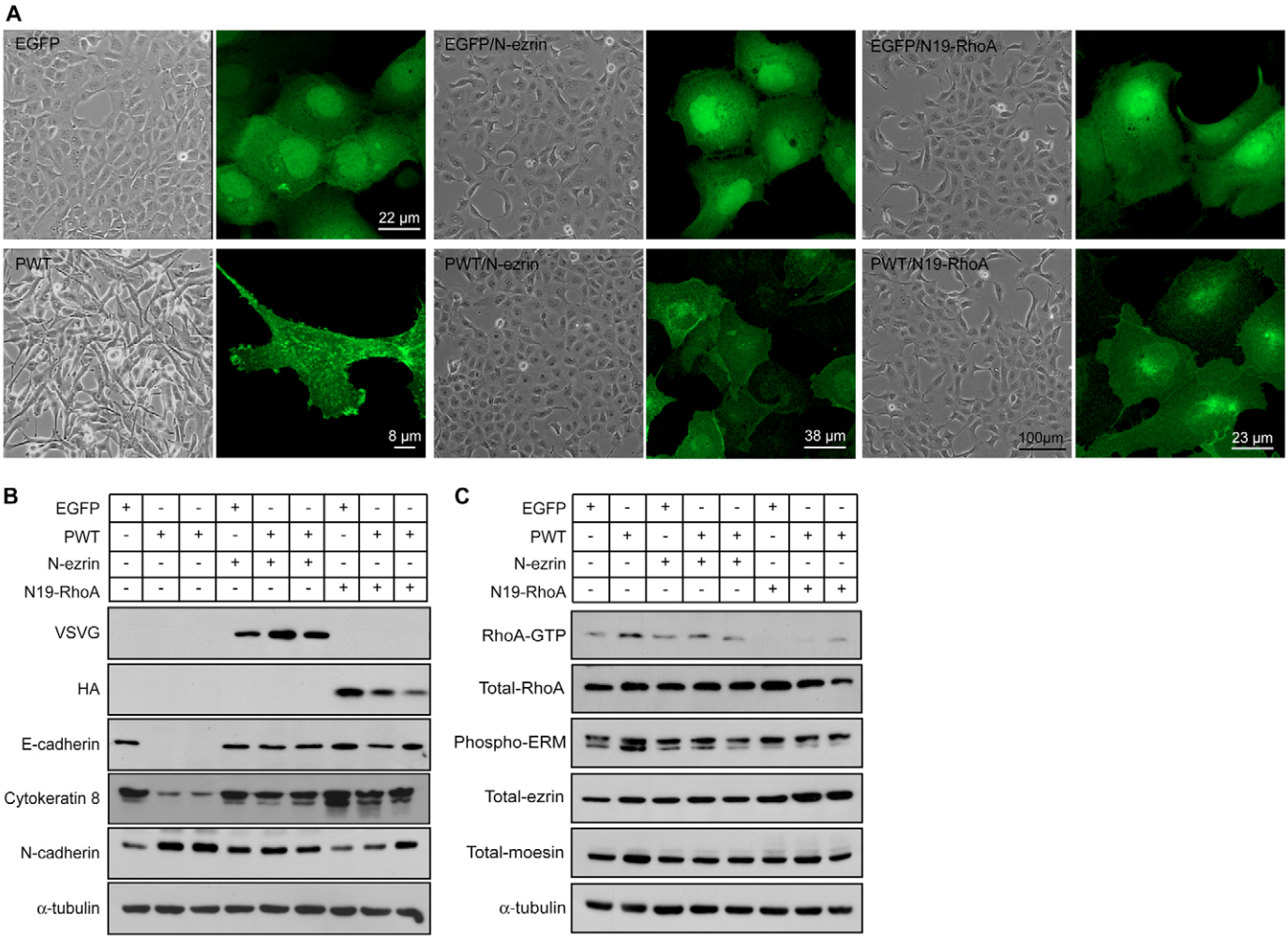

Fig. 8. Dominant-negative effects of N19RhoA and of N-terminal domain of ezrin (N-ezrin) in podoplanin-induced EMT. (A) Phase-contrast micrographs and confocal fluorescence detection of podoplanin in MDCK cells cotransfected with EGFP-tagged PWT and N-ezrin or N19RhoA. Control cells expressing EGFP alone, EGFP/N-ezrin and EGFP/N19RhoA are also shown. Confocal images are maximum projections of horizontal optical sections through the whole depth of the transfectants. (B) Western blot analysis of N-ezrin (VSVG), N19RhoA (HA) and differentiation-related proteins in MDCK cell transfectants. N-ezrin and N19RhoA expression was determined by using antibodies against their respective tags. (C) N-ezrin and N19RhoA inhibits podoplanin-mediated RhoA activation and ERM phosphorylation. The levels of RhoA-GTP relative to the levels of total RhoA and the levels of phospho-ERM relative to the total expression levels of ezrin and moesin are shown. The expression of α-tubulin was determined as a control for protein loading.

cytoplasmic tail of podoplanin (**RK**MSG**R**YSP) is extremely short and binds directly to ezrin and moesin through a cluster of three basic residues (bold). In vivo, the interaction of podoplanin with ezrin appears to be mainly mediated by the juxtamembrane dipeptide RK, because substitution of these two or all three basic residues by uncharged polar amino acids (PCTQN or PCTQN.N) had the same effect as deletion of the entire cytoplasmic tail (PΔCT) in blocking podoplanin association with ezrin. By contrast, mutation of the most C-terminal residue R159 (PCT.N) impaired, but did not prevent, podoplanin-ezrin interaction. PΔCT, PCTQN and PCTQN.N were unable to induce RhoA activation and EMT, whereas PCT.N pushed MDCK cells to an intermediate phenotype (the so-called fibroblastoid phenotype) characterized by mixed expression of epithelial (i.e. E-cadherin) and mesenchymal (i.e. N-cadherin) protein markers and by a fibroblast-like morphology and migratory behavior. Overall, these results suggested that podoplanin needs to recruit ERM proteins through the endodomain in order to activate RhoA and promote EMT, and this hypothesis was confirmed by loss-of-function experiments. Suppression of the function of either ezrin or RhoA by the introduction in MDCK cells of a dominant-negative form of any of these proteins blocked podoplanin-induced RhoA activation and EMT. An intriguing question is how podoplanin expression in MDCK cells leads to RhoA activation. We speculate that this could occur by a similar mechanism to that exhibited by the hyaluronan receptor CD44. Hirao and coworkers found that Rho-GDP dissociation inhibitor (Rho-GDI), which sequesters Rho GTPases bound to GDP in the cytoplasm, could be coimmunoprecipitated together with CD44-ERM complexes (Hirao et al., 1996). The binding of Rho-GDI to the exposed N-ERMAD domain of ERM proteins releases RhoA-GDP from the inhibitor, allowing its activation by a GDP-GTP exchange factor (Takahashi et al.,

1997; Takahashi et al., 1998). Thus, podoplanin recruitment of ezrin and/or moesin to the membrane not only would mediate its anchorage to the actin cytoskeleton but also would activate RhoA facilitating EMT. In this regard, it has been shown that ezrin influences the metastatic potential of tumor cell lines, at least in part, through activation of RhoA (Yu et al., 2004). Once activated, RhoA can contribute to stabilize ERM proteins further in an active conformation either by Rock-dependent phosphorylation of a T residue in the C-terminal domain, as shown in this work, or by RhoA-dependent production of PIP_2 (Tsukita and Yonemura, 1999; Ivetic and Ridley, 2004).

A recent report (Wicki et al., 2006) has described podoplanin stimulation of collective cell migration and invasion (in the absence of EMT) in MCF7 breast carcinoma cells. This effect was mediated by the induction of filopodia-like structures in the migrating front, and, surprisingly, involved combined inactivation of RhoA, Rac1 and Cdc42, although only inhibition of RhoA signaling appeared to mediate filopodia formation. These results suggest a direct role of podoplanin in stimulating epithelial cell migration independently of promoting EMT, and are in line with our previous observations suggesting that the extent of podoplanin-mediated phenotypic changes is dependent on the cell type or the state of cellular differentiation. Thus, podoplanin induces filopodia formation in human immortalized HaCaT keratinocytes, but fails to downregulate E-cadherin expression and to promote a complete EMT (Martín-Villar et al., 2005). This is in contrast to the profound phenotypic changes induced by podoplanin in MDCK, a highly sensitive cell line, which undergoes EMT in the presence of different inducers (Gotzman et al., 2004). A major discrepancy with the results of Wicki and co-workers is the fact that, in our hands, podoplanin activates RhoA without affecting Rac1 and Cdc42 activities in both MDCK and HaCaT cells. In MCF7 cells, stimulation of cell migration is associated with RhoA inhibition, whereas the opposite is true in MCDK cells. It is well established that RhoA activation can either inhibit or promote cell migration in distinct cell types (see Ridley, 2004; Lozano et al., 2005). This fact probably reflects a particular organization of the cellular cytoskeleton (microfilaments, microtubules and intermediate filaments) and of adhesion components, as well as a different way for Rho GTPases to coordinately regulate cell migration. As a matter of fact, while the basal level of active RhoA is relatively high in MCF7 cells (Wicki et al., 2006), it is low in MDCK and HaCaT cells compared with the levels of active Rac and Cdc42 (Zondag et al., 2000) (this paper). After all, both situations, i.e. podoplanin stimulation of in vitro cell migration or invasion with and without EMT, are compatible with the in vivo data. In many human carcinomas, podoplanin is coexpressed together with E-cadherin in the invasive front of the tumors (Wicki et al., 2006), but we also found that the presence of podoplanin coincides with the loss of E-cadherin expression in the invasive front of some oral squamous cell carcinomas (Martin-Villar et al., 2005).

Interestingly, epithelial MDCK cells expressing mutant PΔCT consistently showed loose cell-cell contacts and enhanced migratory and invasive abilities in comparison with control cells or cells expressing PCTQN.N and PCTQN. These results suggest that the podoplanin CT domain might contain residues that positively affect the stability of adherens junctions. These residues should be other than those involved in ERM binding or should become functional when the ERM-binding sites are inactivated. This hypothesis is supported by the fact that PCTQN.N, PCTQN and PΔCT mutant proteins are expressed at cell-cell contacts in epithelial MDCK cells. In this regard, Wicki and co-workers observed that the majority of pancreatic carcinomas in a transgenic mouse model (Rip1Podo;Rip1Tag2) with targeted expression of podoplanin in β cells of islets of Langerhans retained E-cadherin expression whereas it was lost in most carcinomas of control mice (Wicki et al., 2006). Yet, at present, we do not have a rational explanation for the unexpected phenotype of PΔCT-MDCK cell transfectants. Other observations related to the phenotypes of MDCK cells expressing PCT.N and PΔEC suggest that podoplanin can influence cell spreading. Both types of fibroblast-like cell transfectants showed smaller focal contacts and fewer stress fibers when compared with well-spread MDCK cells expressing PWT. Since podoplanin appears to be absent from focal contacts and does not associate with stress fibers (Scholl et al., 1999), these observations suggest that the ectodomain, and possibly its interaction with extracellular components could affect the dynamics of cell to substratum adhesion. It has been found that podoplanin induces platelet aggregation through the EC domain (Kato et al., 2003; Kaneko et al., 2006). In addition, we have obtained experimental evidence indicating that podoplanin interacts with extracellular matrix components (unpublished results). These data suggest an adhesive role for this glycoprotein. The interaction of podoplanin with extracellular components might be mechanically transmitted to the actin cytoskeleton through the cytoplasmic tail, as occurs with most, if not all, membrane adhesion receptors (Brunton et al., 2004). Thus, the inability of podoplanin to bind to extracellular components (PΔEC) or the diminished or inappropriate interaction of podoplanin with intracellular molecules involved in actin dynamics (PCT.N) could affect the dynamics of focal adhesions.

A final point brought to the discussion is the fact that although podoplanin-induced EMT is dependent on the interaction of the cytoplasmic tail with ERM proteins and then with the cytoskeleton, the localization of podoplanin at cell-surface protrusions requires neither the endodomain nor the ectodomain, pointing to the transmembrane domain as the structural element responsible for the presence of podoplanin within this particular membrane region. This might be mediated by the association of the podoplanin TM domain with lipid rafts, as occurs with CD44 (Perschl et al., 1995). It has been proposed that protrusive motility at the cell surface might be regulated through the local accumulation of raft domains enriched in PIP_2 (Yin and Janmey, 2003; Golub and Caroni, 2005). The implication of the podoplanin TM domain in the localization of this glycoprotein at cell-surface protrusions and its possible interaction with lipid rafts is currently being investigated.

Materials and Methods

Constructs

Constructs for GST fusion proteins of the podoplanin CT were generated by synthesizing each cDNA carrying *Eco*RI and *Xho*I restriction sites to facilitate subcloning into the pGEX-4T1 vector (Amersham Biosciences). cDNAs for the CT of CD44 and full-length ezrin or its N-ERMAD region (residues 1-310) were obtained by PCR amplification from HT1080 and HeLa cells, respectively. Constructs for GST-full-length moesin and its N-ERMAD region were a gift from Francisco Sánchez-Madrid (Hospital de la Princesa, Madrid, Spain) and constructs for tagged dominant-negative forms of ezrin (N-ezrin) and RhoA (N19RhoA) were

kindly provided by Paul Mangeat (University of Montpellier, France) and Piero Crespo (Instituto de Investigaciones Biomédicas, Madrid, Spain), respectively. Ezrin tagged with ECFP at the C-terminus, EYFP- and EGFP-tagged podoplanin constructs were obtained by PCR amplification using primers that carry both the desired mutation (in the case of podoplanin mutant constructs) and a convenient restriction site to facilitate subcloning into pECFP-N1, pEYFP-N1, pEGFP-N1 and pEGFP-C1 vectors. Oligonucleotides used for amplification of all these constructs are described in Table S1 in supplementary material. All PCR-derived constructs were sequenced in an ABI Prism 377 system (Perkin Elmer) to confirm that nucleotide sequences were correct.

RT-PCR analysis

RT-PCR analysis was carried out as described previously (Martín-Villar et al., 2005). Canine PCR products were obtained after 30-35 cycles of amplification with an annealing temperature of 60-65°C. Primer sequences for canine E-cadherin (*CDH1*), *Snail* and glyceraldehyde-3-phosphate dehydrogenase (*GAPDH*) have been described elsewhere (Peinado et al., 2003). For canine *Slug* the following oligonucleotides were used: 5′-AGTGATTATTTCCCCATATCTCTATGA-3′ and 5′-GTAGTCTTTCCTCTTCATCACTAATGG-3′ (amplifies a fragment of 300 bp).

Cell culture conditions and cDNA transfections

Cell culture conditions and transfection procedures were as previously described (Martín-Villar et al., 2005). MDCK cell transfectants were selected in 0.5 mg/ml of G418 (Promega) for 2 weeks. Individual clones were isolated with cloning rings. For FRET experiments, MDCK cells at 60-70% confluence were cotransfected with Ezrin-ECFP and EYFP-tagged podoplanin constructs. Cells selected in 0.5 mg/ml of G418 for 10 days were plated onto coverslips, fixed with 3.7% formaldehyde and mounted on Mowiol. The Rock inhibitor Y27632 (Calbiochem) and the cell permeable recombinant C3 transferase (Cytoskeleton) were added to the cell cultures at 5 μM and 2 μg/ml, respectively. For treatments with C3 transferase, a 0.1% concentration of serum was used in the cultures.

In vitro binding assay between ERM and GST fusion proteins

GST and GST fusion proteins were produced in *E. coli* BL21 cells as described (Sander et al., 1998). Pure dialyzed GST and GST fusion proteins were bound to CNBr-activated Sepharose (Amersham Pharmacia Biotech) according to the manufacturer's instructions. Approximately 1 nmol of pure dialyzed full-length ezrin or moesin and their respective N-ERMADs were mixed with 500 pmol of fusion proteins bound to Sepharose in a final volume of 500 μl of binding buffer (50 mM Tris-HCl pH 7.5, 1 mM $MgCl_2$, 100 mM NaCl, 0.4% Triton X-100), in the presence or absence of 50 μg/ml PIP2 (Sigma-Aldrich), and incubated for 30 minutes at room temperature. Beads were then washed six times in binding buffer, boiled in Laemmli buffer, and bound ERMs analyzed by western blotting.

Western blot analysis and antibodies

Cell lysates were obtained in RIPA buffer (0.1% SDS, 0.5% sodium deoxycholate, 1% NP-40, 150 mM NaCl, 50 mM Tris-HCl pH 7.5 and a cocktail of protease inhibitors) and analyzed by western blotting. Polyclonal antibodies against ezrin and moesin were kindly provided by Paul Mangeat; anti-phospho-ERM antibody was from Cell Signaling Technology; antibodies for RhoA and HA were from Santa Cruz Biotechnology; antibodies for EGFP, fibronectin, VSVG and α-tubulin (mAb DM1A) were from Sigma-Aldrich; mAbs for p120ctn, β-catenin (C19220), Rac1 and Cdc42 were from BD Biosciences; and mAbs for N-cadherin, vimentin and cytokeratin 8 from Zymed Laboratories, Dako and Progen, respectively. Horseradish-peroxidase-conjugated sheep anti-mouse (Amersham Biosciences), goat anti-rat (Pierce) and goat anti-rabbit (Nordic) IgGs were used as secondary antibodies.

Immunofluorescence analysis and time-lapse confocal microscopy

Detection of E-cadherin and β-catenin was performed on confluent cells grown on glass coverslips and fixed in cold methanol using mAbs 4A2C7 (Zymed) and C19220 (BD Biosciences), respectively. Detection of vimentin, fibronectin, ezrin, vinculin, RhoA, Rac1 and F-actin was performed in cells fixed with 3.7% formaldehyde in PBS and permeabilized with 0.05% Triton X-100. The mAb 3C12 (Sigma-Aldrich) was used for detection of ezrin. For F-actin staining, phalloidin coupled to Alexa Fluor 594 (Molecular Probes) was used. Secondary antibodies were Alexa Fluor 594-labeled anti-rabbit or anti-mouse IgGs (Molecular Probes). Staining of nuclei was performed in a 1 μg/ml solution of 4′,6-diamino-2-phenilindole (DAPI; Sigma-Aldrich). Confocal laser-scanning microscopy was performed in a Leica TCS-SP2 microscope (Leica Microsystems, Heidelberg, Germany). Images were taken using a 63× (NA 1.32) oil-immersion objective and assembled using Leica Confocal Software 2.0.

For in vivo podoplanin pre-embedding staining, subconfluent cells grown on glass coverslips were incubated in DMEM containing 25 mM HEPES and 1% BSA (buffer D) for 15 minutes, and stained with rabbit anti-podoplanin (Martín-Villar et al., 2005) or rabbit anti-EGFP A11122 (Molecular Probes) antibodies at 1:100 dilution in buffer D for 1 hour at 4°C. Alexa Fluor 594-labeled anti-rabbit IgG (Molecular Probes) was used as secondary antibody. Coverslips were then fixed with 3.7% paraformaldehyde in buffer D, mounted on Mowiol and examined in a Leica TCS-SP2 confocal scanning laser microscope.

For time-lapse confocal microscopy, cells grown at low confluence on glass-bottom dishes (Lab-Tek® II) were maintained at 37°C in a 5% CO_2 atmosphere using an incubation system. Confocal series of fluorescence images (22 slices of 0.5 μm) were simultaneously obtained with a 63×/1.32 oil immersion objective every 10 minutes intervals for 4 hours. Images were processed and assembled into movies using the Leica Confocal Software 2.0 and Adobe Premiere Pro 1.5 software.

FRET by acceptor photobleaching

FRET was examined by the acceptor photobleaching method with EYFP-tagged podoplanin and ECFP-tagged ezrin incorporated into MDCK cells. A Leica TCS-SP2 confocal scanning laser microscope equipped with a 63×/1.32 oil-immersion lens was used. Energy transfer was detected as an increase in donor fluorescence (CFP) after photobleaching of the acceptor molecules (EYFP). ECFP and EYFP emission signals were collected before and after EYFP photobleaching by using the 458 nm or 514 nm laser lines, respectively. Images were background corrected and the $FRET_{eff}$ was calculated for each pixel from the increase of the donor fluorescence: $FRET_{eff}=(D_{post}-D_{pre})/D_{post}$; for all $D_{post}>D_{pre}$, where D_{pre} and D_{post} are the donor fluorescence intensities before and after acceptor photobleaching, respectively.

Wound healing assay and time-lapse video microscopy

The migratory behavior of cell transfectants was analyzed in an in vitro wound-healing assay, as described previously (Scholl et al., 1999). Wounded cell cultures were maintained at 37°C in a 5% CO_2 atmosphere using an incubation system. Images of the wounds were acquired every 10 minutes for 12 hours using a Zeiss Axiovert 135 TV inverted microscope equipped with a Digital JVC video camera. Quantification of migrated cells was done by measuring the number of pixels in the wounded area at different times using Adobe® Photoshop®. Images and videos were assembled using Analysis® 3.2 (Soft Imaging System) and Adobe Premiere Pro 1.5 software.

In vitro invasion assay

Cells (2.5×10^4) were suspended in 500 μl DMEM and loaded onto the upper compartment of BD BioCoat™ Matrigel™ Invasion Chamber (BD Biosciences). 5% FBS was used as a chemoattractant in the lower compartment. Cell invasion was analyzed by detection of EGFP using a Leica TCS-SP2 confocal microscope equipped with a 20×/0.70 and 63×/1.32 oil immersion lens. Fluorescence intensity profiles were obtained by image analysis using Leica Confocal Software 2.0.

RhoA, Rac1 and Cdc42 activity assays

The level of active RhoA (RhoA-GTP) in cell lysates was measured using a GST fusion protein with the RhoA-binding domain of Rhotekin (GST-C21). For Rac1 and Cdc42 activities, a GST fusion protein of the binding domain of PAK (GST-PAK) was used. Assays were performed as described by Sander and co-workers (Sander et al., 1998).

Statistics

Data are presented as mean ± s.e.m. Significance was determined using the Student's *t*-test. All statistical analyses were performed using GraphPad Prism 4.0 software.

We thank Francisco Sánchez-Madrid, Piero Crespo and Paul Mangeat for their useful gifts of antibodies or plasmids. We also thank David Sarrio for his help with p120 ctn expression studies, Paloma Ordóñez for her help with dominant-negative RhoA studies and Jaime Renart for critical reading of the manuscript. This work was supported by grants: SAF2004-04902 from the Ministry of Education and Science (MEC), GR/SAL/0871/2004 from the Autonomous Community of Madrid (CAM) and RTICCC CO3/10 from the 'Instituto de Salud Carlos III' (FIS) of Spain. E.M.-V. and M.M.Y. were the recipients of a postgraduate I3P fellowship from the Spanish Research Council (CSIC) and an MEC predoctoral fellowship, respectively.

References

Batlle, E., Sancho, E., Franci, C., Dominguez, D., Monfar, M., Baulida, J. and Garcia De Herreros, A. (2000). The transcription factor snail is a repressor of E-cadherin gene expression in epithelial tumour cells. *Nat. Cell Biol.* **2**, 84-89.

Bhowmick, N. A., Ghiassi, M., Bakin, A., Aakre, M., Lundquist, C. A., Engel, M. E., Arteaga, C. L. and Moses, H. L. (2001). Transforming growth factor-beta1 mediates epithelial to mesenchymal transdifferentiation through a RhoA-dependent mechanism. *Mol. Biol. Cell* **12**, 27-36.

Bissell, M. J. and Radisky, D. (2001). Putting tumours in context. *Nat. Rev. Cancer* **1**, 46-54.

Bolós, V., Peinado, H., Perez-Moreno, M. A., Fraga, M. F., Esteller, M. and Cano, A. (2003). The transcription factor Slug represses E-cadherin expression and induces epithelial to mesenchymal transitions: a comparison with Snail and E47 repressors. *J. Cell Sci.* **116**, 499-511.

Breiteneder-Geleff, S., Matsui, K., Soleiman, A., Meraner, P., Poczewski, H., Kalt, R., Schaffner, G. and Kerjaschki, D. (1997). Podoplanin, novel 43-kd membrane protein of glomerular epithelial cells, is down-regulated in puromycin nephrosis. *Am. J. Pathol.* **151**, 1141-1152.

Breiteneder-Geleff, S., Soleiman, A., Kowalski, H., Horvat, R., Amann, G., Kriehuber, E., Diem, K., Weninger, W., Tschachler, E., Alitalo, K. et al. (1999). Angiosarcomas express mixed endothelial phenotypes of blood and lymphatic capillaries: podoplanin as a specific marker for lymphatic endothelium. *Am. J. Pathol.* **154**, 385-394.

Bretscher, A., Edwards, K. and Fehon, R. G. (2002). ERM proteins and merlin: integrators at the cell cortex. *Nat. Rev. Mol. Cell Biol.* **3**, 586-599.

Brunton, V. G., MacPherson, I. R. and Frame, M. C. (2004). Cell adhesion receptors, tyrosine kinases and actin modulators: a complex three-way circuitry. *Biochim. Biophys. Acta* **1692**, 121-144.

Cano, A., Perez-Moreno, M. A., Rodrigo, I., Locascio, A., Blanco, M. J., del Barrio, M. G., Portillo, F. and Nieto, M. A. (2000). The transcription factor snail controls epithelial-mesenchymal transitions by repressing E-cadherin expression. *Nat. Cell Biol.* **2**, 76-83.

Cavallaro, U. and Christofori, G. (2004). Multitasking in tumor progression: signaling functions of cell adhesion molecules. *Ann. N. Y. Acad. Sci.* **1014**, 58-66.

Chu, A. Y., Litzky, L. A., Pasha, T. L., Acs, G. and Zhang, P. J. (2005). Utility of D2-40, a novel mesothelial marker, in the diagnosis of malignant mesothelioma. *Mod. Pathol.* **18**, 105-110.

Crepaldi, T., Gautreau, A., Comoglio, P. M., Louvard, D. and Arpin, M. (1997). Ezrin is an effector of hepatocyte growth factor-mediated migration and morphogenesis in epithelial cells. *J. Cell Biol.* **138**, 423-434.

Farooqui, R. and Fenteany, G. (2005). Multiple rows of cells behind an epithelial wound edge extend cryptic lamellipodia to collectively drive cell-sheet movement. *J. Cell Sci.* **118**, 51-63.

Gandarillas, A., Scholl, F. G., Benito, N., Gamallo, C. and Quintanilla, M. (1997). Induction of PA2.26, a cell-surface antigen expressed by active fibroblasts, in mouse epidermal keratinocytes during carcinogenesis. *Mol. Carcinog.* **20**, 10-18.

Golub, T. and Caroni, P. (2005). PI(4,5)P2-dependent microdomain assemblies capture microtubules to promote and control leading edge motility. *J. Cell Biol.* **169**, 151-165.

Gotzmann, J., Mikula, M., Eger, A., Schulte-Hermann, R., Foisner, R., Beug, H. and Mikulits, W. (2004). Molecular aspects of epithelial cell plasticity: implications for local tumor invasion and metastasis. *Mutat. Res.* **566**, 9-20.

Hirao, M., Sato, N., Kondo, T., Yonemura, S., Monden, M., Sasaki, T., Takai, Y., Tsukita, S. and Tsukita, S. (1996). Regulation mechanism of ERM (ezrin/radixin/moesin) protein/plasma membrane association: possible involvement of phosphatidylinositol turnover and Rho-dependent signaling pathway. *J. Cell Biol.* **135**, 37-51.

Ivetic, A. and Ridley, A. J. (2004). Ezrin/radixin/moesin proteins and Rho GTPase signalling in leucocytes. *Immunology* **112**, 165-176.

Kaneko, M. K., Kato, Y., Kitano, T. and Osawa, M. (2006). Conservation of a platelet activating domain of Aggrus/podoplanin as a platelet aggregation-inducing factor. *Gene* **378**, 52-57.

Kato, Y., Fujita, N., Kunita, A., Sato, S., Kaneko, M., Osawa, M. and Tsuruo, T. (2003). Molecular identification of Aggrus/T1alpha as a platelet aggregation-inducing factor expressed in colorectal tumors. *J. Biol. Chem.* **278**, 51599-51605.

Kato, Y., Sasagawa, I., Kaneko, M., Osawa, M., Fujita, N. and Tsuruo, T. (2004). Aggrus: a diagnostic marker that distinguishes seminoma from embryonal carcinoma in testicular germ cell tumors. *Oncogene* **23**, 8552-8556.

Kato, Y., Kaneko, M., Sata, M., Fujita, N., Tsuruo, T. and Osawa, M. (2005). Enhanced expression of Aggrus (T1alpha/podoplanin), a platelet-aggregation-inducing factor in lung squamous cell carcinoma. *Tumour Biol.* **26**, 195-200.

Kotani, M., Tajima, Y., Osanai, T., Irie, A., Iwatsuki, K., Kanai-Azuma, M., Imada, M., Kato, H., Shitara, H., Kubo, H. et al. (2003). Complementary DNA cloning and characterization of RANDAM-2, a type I membrane molecule specifically expressed on glutamatergic neuronal cells in the mouse cerebrum. *J. Neurosci. Res.* **73**, 603-613.

Legg, J. W. and Isacke, C. M. (1998). Identification and functional analysis of the ezrin-binding site in the hyaluronan receptor, CD44. *Curr. Biol.* **8**, 705-708.

Lozano, E., Betson, M. and Braga, V. M. (2003). Tumor progression: small GTPases and loss of cell-cell adhesion. *BioEssays* **25**, 452-463.

Martín-Villar, E., Scholl, F. G., Gamallo, C., Yurrita, M. M., Munoz-Guerra, M., Cruces, J. and Quintanilla, M. (2005). Characterization of human PA2.26 antigen (T1alpha-2, podoplanin), a small membrane mucin induced in oral squamous cell carcinomas. *Int. J. Cancer* **113**, 899-910.

Matsubayashi, Y., Ebisuya, M., Honjoh, S. and Nishida, E. (2004). ERK activation propagates in epithelial cell sheets and regulates their migration during wound healing. *Curr. Biol.* **14**, 731-735.

Matsui, T., Maeda, M., Doi, Y., Yonemura, S., Amano, M., Kaibuchi, K. and Tsukita, S. (1998). Rho-kinase phosphorylates COOH-terminal threonines of ezrin/radixin/moesin (ERM) proteins and regulates their head-to-tail association. *J. Cell Biol.* **140**, 647-657.

Peinado, H., Quintanilla, M. and Cano, A. (2003). Transforming growth factor beta-1 induces snail transcription factor in epithelial cell lines: mechanisms for epithelial mesenchymal transitions. *J. Biol. Chem.* **278**, 21113-21123.

Perschl, A., Lesley, J., English, N., Hyman, R. and Trowbridge, I. S. (1995). Transmembrane domain of CD44 is required for its detergent insolubility in fibroblasts. *J. Cell Sci.* **108**, 1033-1041.

Ramirez, M. I., Millien, G., Hinds, A., Cao, Y., Seldin, D. C. and Williams, M. C. (2003). T1alpha, a lung type I cell differentiation gene, is required for normal lung cell proliferation and alveolus formation at birth. *Dev. Biol.* **256**, 61-72.

Ridley, A. J. (2001). Rho GTPases and cell migration. *J. Cell Sci.* **114**, 2713-2722.

Rishi, A. K., Joyce-Brady, M., Fisher, J., Dobbs, L. G., Floros, J., VanderSpek, J., Brody, J. S. and Williams, M. C. (1995). Cloning, characterization, and development expression of a rat lung alveolar type I cell gene in embryonic endodermal and neural derivatives. *Dev. Biol.* **167**, 294-306.

Sahai, E. and Marshall, C. J. (2002a). RHO-GTPases and cancer. *Nat. Rev. Cancer* **2**, 133-142.

Sahai, E. and Marshall, C. J. (2002b). ROCK and Dia have opposing effects on adherens junctions downstream of Rho. *Nat. Cell Biol.* **4**, 408-415.

Sander, E. E., van Delft, S., ten Klooster, J. P., Reid, T., van der Kammen, R. A., Michiels, F. and Collard, J. G. (1998). Matrix-dependent Tiam1/Rac signaling in epithelial cells promotes either cell-cell adhesion or cell migration and is regulated by phosphatidylinositol 3-kinase. *J. Cell Biol.* **143**, 1385-1398.

Sander, E. E., ten Klooster, J. P., van Delft, S., van der Kammen, R. A. and Collard, J. G. (1999). Rac downregulates Rho activity: reciprocal balance between both GTPases determines cellular morphology and migratory behavior. *J. Cell Biol.* **147**, 1009-1022.

Sarrio, D., Perez-Mies, B., Hardisson, D., Moreno-Bueno, G., Suarez, A., Cano, A., Martin-Perez, J., Gamallo, C. and Palacios, J. (2004). Cytoplasmic localization of p120ctn and E-cadherin loss characterize lobular breast carcinoma from preinvasive to metastatic lesions. *Oncogene* **23**, 3272-3283.

Schacht, V., Ramirez, M. I., Hong, Y. K., Hirakawa, S., Feng, D., Harvey, N., Williams, M., Dvorak, A. M., Dvorak, H. F., Oliver, G. et al. (2003). T1alpha/podoplanin deficiency disrupts normal lymphatic vasculature formation and causes lymphedema. *EMBO J.* **22**, 3546-3556.

Schacht, V., Dadras, S. S., Johnson, L. A., Jackson, D. G., Hong, Y. K. and Detmar, M. (2005). Up-regulation of the lymphatic marker podoplanin, a mucin-type transmembrane glycoprotein, in human squamous cell carcinomas and germ cell tumors. *Am. J. Pathol.* **166**, 913-921.

Scholl, F. G., Gamallo, C., Vilaró, S. and Quintanilla, M. (1999). Identification of PA2.26 antigen as a novel cell-surface mucin-type glycoprotein that induces plasma membrane extensions and increased motility in keratinocytes. *J. Cell Sci.* **112**, 4601-4613.

Scholl, F. G., Gamallo, C. and Quintanilla, M. (2000). Ectopic expression of PA2.26 antigen in epidermal keratinocytes leads to destabilization of adherens junctions and malignant progression. *Lab. Invest.* **80**, 1749-1759.

Takahashi, K., Sasaki, T., Mammoto, A., Takaishi, K., Kameyama, T., Tsukita, S. and Takai, Y. (1997). Direct interaction of the Rho GDP dissociation inhibitor with ezrin/radixin/moesin initiates the activation of the Rho small G protein. *J. Biol. Chem.* **272**, 23371-23375.

Takahashi, K., Sasaki, T., Mammoto, A., Hotta, I., Takaishi, K., Imamura, H., Nakano, K., Kodama, A. and Takai, Y. (1998). Interaction of radixin with Rho small G protein GDP/GTP exchange protein Dbl. *Oncogene* **16**, 3279-3284.

Thiery, J. P. (2002). Epithelial-mesenchymal transitions in tumour progression. *Nat. Rev. Cancer* **2**, 442-454.

Tsukita, S. and Yonemura, S. (1999). Cortical actin organization: lessons from ERM(ezrin/radixin/moesin) proteins. *J. Biol. Chem.* **274**, 34507-34510.

Wetterwald, A., Hoffstetter, W., Cecchini, M. G., Lanske, B., Wagner, C., Fleisch, H. and Atkinson, M. (1996). Characterization and cloning of the E11 antigen, a marker expressed by rat osteoblasts and osteocytes. *Bone* **18**, 125-132.

Wicki, A., Lehembre, F., Wick, N., Hanfusch, B., Kerjaschki, D. and Christofori, G. (2006). Tumor invasion in the absence of epithelial-mesenchymal transition: podoplanin-mediated remodelling of the actin cytoskeleton. *Cancer Cell* **9**, 261-272.

Williams, M. C., Cao, Y., Hinds, A., Rishi, A. K. and Wetterwald, A. (1996). T1 alpha protein is developmentally regulated and expressed by alveolar type I cells, choroid plexus, and ciliary epithelia of adult rats. *Am. J. Respir. Cell Mol. Biol.* **14**, 577-585.

Yin, H. L. and Janmey, P. A. (2003). Phosphoinositide regulation of the actin cytoskeleton. *Annu. Rev. Physiol.* **65**, 761-789.

Yonemura, S., Hirao, M., Doi, Y., Takahashi, N., Kondo, T., Tsukita, S. and Tsukita, S. (1998). Ezrin/radixin/moesin (ERM) proteins bind to a positively charged amino acid cluster in the juxta-membrane cytoplasmic domain of CD44, CD43, and ICAM-2. *J. Cell Biol.* **140**, 885-895.

Yu, Y., Khan, J., Khanna, C., Helman, L., Meltzer, P. S. and Merlino, G. (2004). Expression profiling identifies the cytoskeletal organizer ezrin and the developmental homeoprotein Six-1 as key metastatic regulators. *Nat. Med.* **10**, 175-181.

Zimmer, G., Oeffner, F., Von Messling, V., Tschernig, T., Groness, H. J., Klenk, H. D. and Herrler, G. (1999). Cloning and characterization of gp36, a human mucin-type glycoprotein preferentially expressed in vascular endothelium. *Biochem. J.* **341**, 277-284.

Zondag, G. C., Evers, E. E., ten Klooster, J. P., Janssen, L., van der Kammen, R. A. and Collard, J. G. (2000). Oncogenic Ras downregulates Rac activity, which leads to increased Rho activity and epithelial-mesenchymal transition. *J. Cell Biol.* **149**, 775-782.